MSc in Photonics

PHOTONICS**BCN**

Universitat Politècnica de Catalunya (UPC)
Universitat Autònoma de Barcelona (UAB)
Universitat de Barcelona (UB)
Institut de Ciències Fotòniques (ICFO)

http://www.photonicsbcn.eu

Master in Photonics

MASTER THESIS WORK

Optical control of thermal diffusion in phase change materials

Daniel Pérez Salinas

Supervised by Prof. Simon Wall, (ICFO)

Presented on date 9th September 2016

Registered at

Escola Tècnica Superior d'Enginyeria de Telecomunicació de Barcelona

Optical control of thermal diffusion in phase change materials

Daniel Prez Salinas

ICFO-The Institute of Photonic Sciences, Av. Carl Friedrich Gauss, 3, 08860, Castelldefels, Barcelona - SPAIN

E-mail: dani.p.salinas@gmail.com

September 2016

Abstract. The long term crystallization of amorphous $Ge_2Sb_2Te_5$ (GST) induced by femtosecond laser pulses has been numerically and experimentally studied. Simulations of the evolution of temperature and crystalline fraction after a single laser pulse in a 100nm layer of GST were done for the normal and lateral directions for different layer stacks and beam profiles. The effect of lateral thermal diffusion was determined to be negligible as a result of normal diffusion and the crystallization requirements limiting the phase change dynamics to a maximum of 2 ns after thermalization. Experimental confirmation was achieved by correlating the top-hat beam profile of the pulses with the crystalline mark induced in the GST.

1. Introduction

Phase change materials (PCMs) based on alloys of Ge, Sb and Te have a variety of interesting scientific and technological properties. These materials can be easily, rapidly and reversibly switched between two solid states, one being ordered-crystalline and the other disordered-amorphous.

The crystallographic and amorphous states show a large difference in the optical and electronic properties of the PCMs and makes them suitable for a wide range of applications such as optical data storage, non-voltatile memory, optical modulation and biologically-inspired computing. The large optical contrast is attributed to the alignment of p-orbitals over next-nearest neighbors present in the crystalline state. This is known as resonant bonding and result in an enhancement of the optical matrix elements and therefore the optical propierties. In the amorphous phase the p-orbitals are no longer aligned meanwhile the local arrangement is still similar to the crystalline state.

Switching between states is achieved by a heat-quench cycle, usually laser- or current- induced.In the context of the prototypical PCM, $Ge_2Sb_2Te_3$ (GST), it has been

experimentally verified that the change in the optical properties can happen before the lattice amorphization in a non-equilibrium situation [11]. However, the long term state will be determined by the equilibrium structural transition resulting from thermal dynamics. This long term state is crucial for applications and thermal dynamics in phase change materials is currently receiving much attention [3],[2],[4],[7]. One of the aspects that often has the spotlight is how precisely can the phase change region be engineered. Having full control on the boundaries of the phase change is desirable in order to benefit from the possibilites offered by spatial beam shaping. This would be useful, for instance, for obtaining greater fill factors for modulators or memories or different plasmonic structures [9],[5]. The physical effect that could limit this degree of control is thermal diffusion. Recently, different views on the effect of diffusion have been published. Some authors defend that diffusion does indeed have significant impact on phase change spatial resolution [1], while others state the opposite [10].

In this work, thermal diffusion and crystallization dynamics are studied numerically and experimentally in order to check wether if thermal diffusion is or could be a limiting factor in mark resolution.

2. Heat diffusion and crystallization model

To predict the amount of crystallization in amorphous GST after a laser pulse it is necessary to calculate the temperature profile induced within the film and its spatial variation over time.

When irradiating the sample with femtosecond laser pulses it is known [11] that crystallization occurs after the end of the pulse irradiation and on a timescale commensurate with the thermalization timescale (nanoseconds)in GST. Therefore, we can model the laser pulses as an instant deposition of heat within the GST. Moreover, the phonon mean free path for both crystalline and amorphous GST is around 0.20 nm [6] and also amorphous GST is known to be a non-metal from a heat diffusion point of view,which means that thermal transport is mainly dictated by phonons, validating the description of the temperature evolution with the equilibrium and macroscopic diffusion equation, that for a static medium is given by:

$$\frac{\partial T(z,r,t)}{\partial t} = D(z,r)\nabla^2 T(r,z,t) + \nabla D(z,r)\nabla T(r,z,t) \tag{1}$$

Where z is the direction parallel to the laser incidence and r is the direction normal to z. In Figure 1 the geometry of the model is shown. $D(z,r)$ is the thermal diffusivity $D(z,r) = k(z,r)/\rho C_p$ where $k(z,r)$, ρ and C_p are the thermal conductivity, density and heat capacity per unit mass respectively. It is important in our model to emphasize the spatial inhomogeneity of the thermal diffusivity since it will represent the thermal propierties both the structure of our sample stack and also the shape of the crystalline

regions. In order to solve the inhomogenous diffusion equation, a direct method based on finite differences described in [8] will be used.

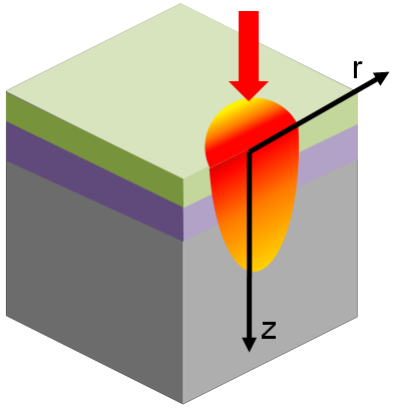

Figure 1. Geometry of the system. The red arrow indicates the direction of the laser beam.

The heat source, the laser, is modelled as an instant deposition of heat in a given time. Its profile will be determined by the beam power, geometry and the sample stack material parameters. This initial temperature is given by

$$T(z,r,t=0) = T_0 + (1-R)\frac{\alpha}{C\rho}I(r)\exp(-\alpha z) \tag{2}$$

Where T_0 is the ambient temperature, R is the reflection coefficient of the stack, α is the absorption coefficient and $I(r)$ is the intensity distribution of the pulse. In the case of a homogeneous intensity distribution it can be written as E/A, being E the pulse energy and A the beam area.

Crystalline GST has two stable structures: cubic and hexagonal. In laser induced crystallization the cubic phase dominates, with the hexagonal appearing seldom and so, it will be neglected. The rate of crystallization can be described by a Arrhenius-type first-order rate equation [6].

$$\frac{\partial\chi(z,r,t)}{\partial t} = [1-\chi(z,r,t)]A_c\exp[\frac{-E_c}{k_BT(z,r)}] \tag{3}$$

Where $\chi(z,r,t)$ is the crystalline volume fraction at a given position and time and has values between 0 and 1, A_c is the frequency term which contains the effect of time (the longer the sample stays above the activation barrier, the more crystallization), E_c the activation barrier which takes in account how hot does the sample get. GST is known to start crystallizing at 400 K and suffers irreversible melting at temperatures above 892 K [1].This equation can be easily solved.

$$1-\chi(z,r,t) = (1-\chi_0(z,r))exp(-A_c\int_0^t \exp\frac{-E_c}{k_BT(z,r)}dt') \tag{4}$$

Where $\chi_0(z,r)$ is the initial crystalline volume fraction. This equation will be numerically integrated in our simulations of crystallization. In Figure 2 the reaction rate as a function of temperature for different crystalline fractions is shown, showing how, owing to the exponential term, the rate of crystalization only becomes significant near the irreversible melting threshold. Therefore, our work will be made in temperatures higher than 800K.

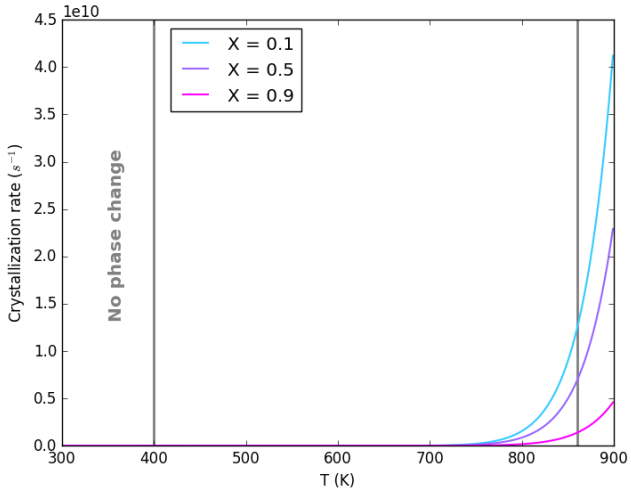

Figure 2. Crystallization rate of GST as a function of temperature for different crystalline fractions.

3. Simulation results

3.1. Z direction

The simulations are done in 1D in order to keep computational requeriments low. Since the two directions in (1) are decoupled [8], reducing it to one dimension is trivial. The scale of the dynamics of each direction were found to be different enough to allow for a complete interpretation of the whole system out of the two results.

The normal direction (z) is the most important to consider when designing functional or experimental material stacks since it allows to engineer a variety of thermal structures with different effects on the overall performance. The following simulations are done for two kinds of sample available in the laboratory at the time of this project. Both samples consist of a 100 nm thick layer of GST deposited on a SiO_2 substrate and one sample has an additional capping layer of Si_3N_4 to prevent oxidization.

The initial conditions are introduced as a temperature profile generated in terms of maximum temperature reached in the surface of the GST layer where the laser beam impinges. In all cases one of the boundaries is air, modelled as a perfect insulator due to the small surface of air molecules in contact with the solid materials and also our

short timescale that limits the magnitude of air displacement. Radiative losses can be neglected. The remaining boundary lies in the substrate. Owing to the thickness of it and the lack of optical absorption this boundary is represented as a heat sink situated a few tens of nanometers into the substrate. Surface thermal resistance in the boundary between GST and the other materials has not been included due to lack of experimental values, nonetheless the thickness of the GST layer ensures that this effect will be unimportant in the GST-SiO_2 boundary. For mathematical simplicity, we consider the phase change to happen after the temperature is allowed to evolve for some nanoseconds, this does not introduce a significant error since we are expecting low crystalline fraction values that will barely change the effective material paremeter.

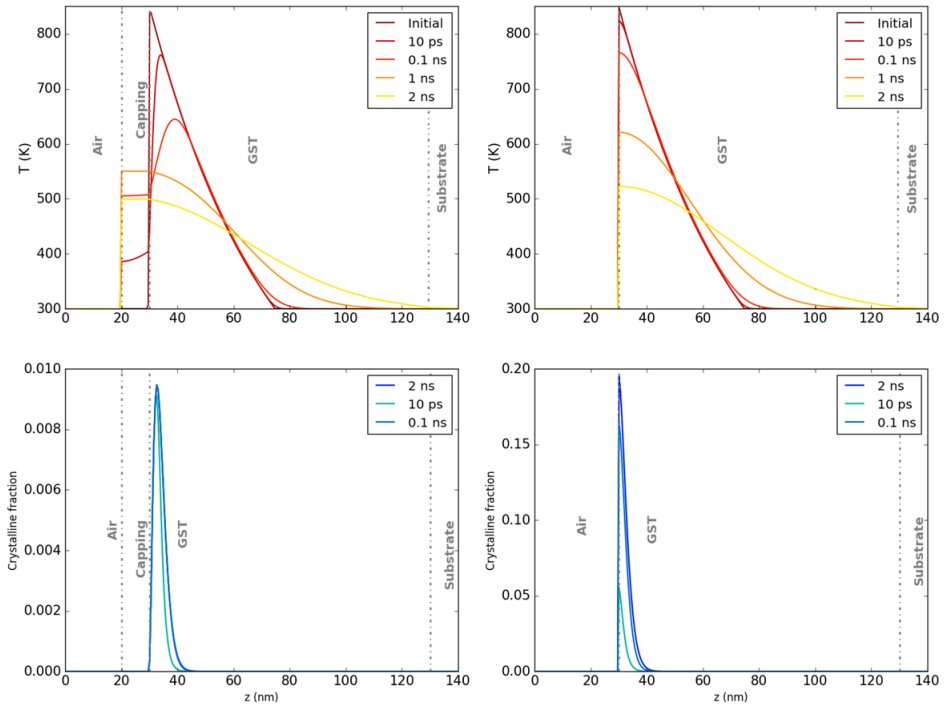

Figure 3. Results of the temperature and crystalline fraction evolution simulations in the z dimension for (a),(c)Sample with capping. (b),(d)Sample without capping. The maximum temperature is 850K in both cases.

In Figure 3 the results for the temperature and crystalline fraction distribution along the z direction at different times after a single laser pulse are shown. It can be seen that in a couple of nanoseconds the temperature drops to values below the activation threshold for crystallization. This suggests, and is confirmed in the crystallization calculations that in a maximum of 2 ns, the phase change dynamics are over. If we took in account that in the real situation part of the energy will flow in the radial direction we can expect the dynamics to finish even earlier.

The simulations also reveal how the capping plays a determinant role in defining the magnitud and distribution of the phase change. As SiN_4 is highly thermally conductive

(10 times higher than GST) the capping layer acts as a heat buffer that prevents the GST layer from remaining in the operational temperatures for long, yielding very low crystalline fraction and moving the maximum of the crystalline phase deep into the layer. In the uncapped version crystalline fraction is two orders of magnitude higher and the crystalline phase forms right in the surface. This suggest the use of an uncapped sample for the experimental measurements. With these results in mind we move onto the other spatial direction.

3.2. R direction

In the transversal direction, the evolution of the temperature profile induced by the full laser pulse is ruled by the same dynamics. In this case, no inhomogeneities are present in the propagation space and therefore the diffusion equation takes a simpler form that can be directly solved via finite differences:

$$\frac{1}{D}\frac{\partial T(r,t)}{\partial t} = \frac{\partial^2 T(r,t)}{\partial r^2} \tag{5}$$

From the results of the simulations in the normal direction we know that only the early (2-3 ns) dynamics are relevant to mark formation however the simulations will comprise of a longer time. In Figure 4 simulation results for different beam shapes are shown. It can be seen that as expected from the higher spatial gradient compared to the normal direction, the temperature profile barely changes in the nanosecond regime. Crystallization rate however is the same as in the previous case and in 2 ns the phase change dynamics end with a crystalline mark that isnt wider than the temperature profile.

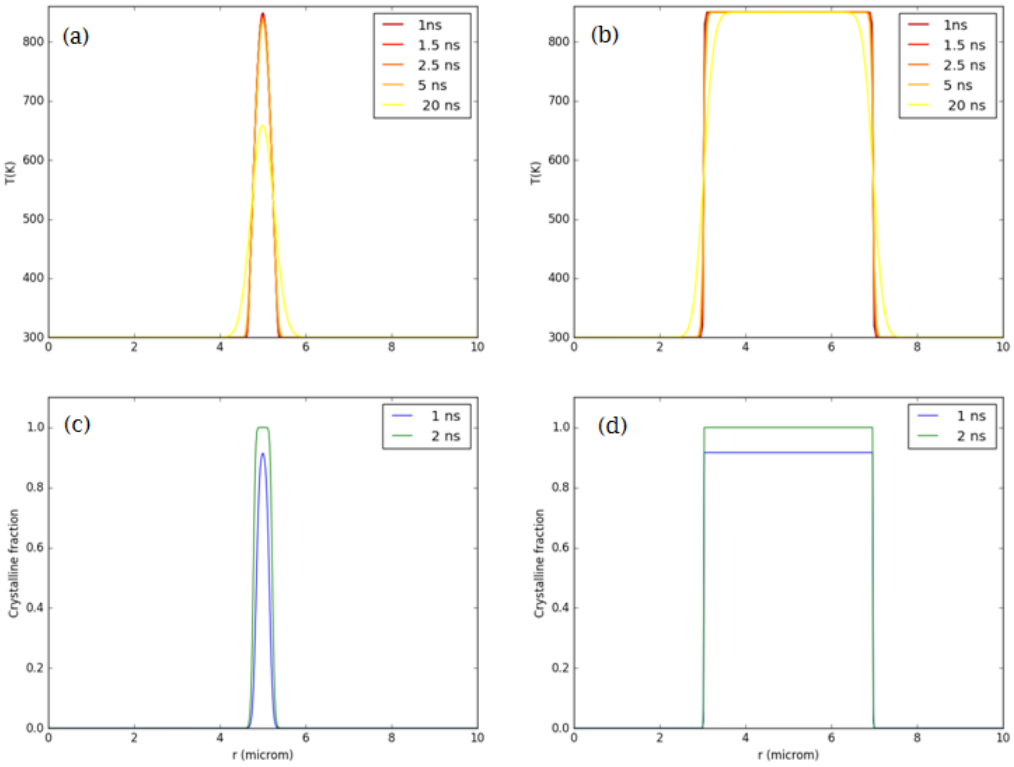

Figure 4. Results of the temperature and crystalline fraction evolution simulations in the r dimension for (a),(c)Gaussian profile. (b),(d)Top-hat profile. The maximum temperature is 850K in both cases.

In the case of the extreme temperature gradient in the ideal top-hat shape a more detailed picture of the edge dynamics is given in Figure 5. In this case the boundary condition in the high-temperature boundary is $T(boundary) = T(boundary - 1)$, which yields accurate results in early diffusion. Again, in the time frame imposed by diffusion in the normal direction, no significative results appear outside the beam area. Again, in 2ns the crystallization process is finished. It is important to keep in mind that the values for crystalline fraction achieved in this simulations do not hold in a real situation and should not be higher than the ones predicted by the simulations in the z direction.

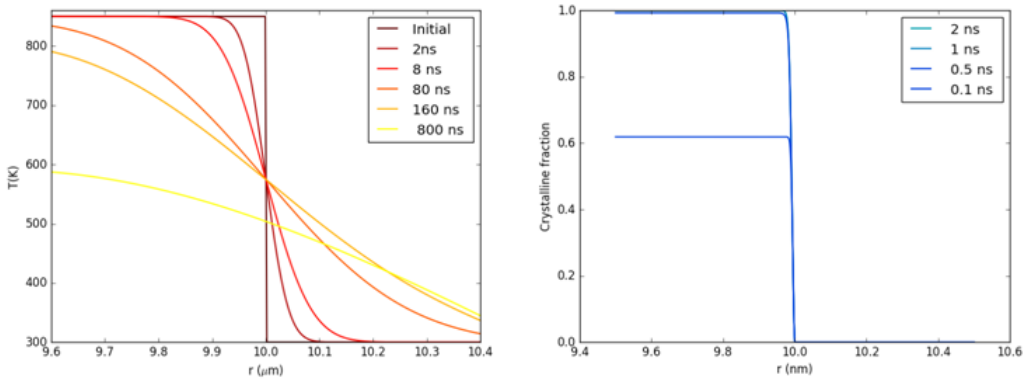

Figure 5. Simulations of lateral (left) heat flow and (right) crystallization at the edge of a top-hat profile in the GST layer for a maximum initial temperature of 850 K

Also featured in Figure 5 are dynamics for much longer times, when the edges have clearly diffused. This could be achievable if the GST layer was grown on a thermal insulator, where diffusion towards the substrate could be minimized. Even in this extreme case there is no crystallization outside the beam area due to the exponential behaviour of the crystallization rate.

4. Experimental setup and results

In order to test wether the beam profile is indeed accurately inscribed in the GST a beam profile that leaves no ambiguity is prefered. In a gaussian beam, specially when not strongly focused, both diffusion of heat from the central region and the 'tailed' nature of the beam would have similar influence in the final shape of the crystalline mark, requiring a more detailed comparison.

With this in mind, we used a square top-hat profile in our experiment. This is a widely used shape due to its availability and variety of applications. In our case it was achieved with the use of a refractive gaussian-to-tophat lens that produces a top-hat profile in the focal plane of a regular convergent lens placed after the beam shaping lens, with the possibility to change the square size by changing the focal lenght of the regular lens.

The light source is given by a Ti:Sapphire laser[central wavelength: 800 nm, bandwidth: 40 nm, pulse energy: 1 mJ, pulse duration: 35 fs, initial beam diameter: 1 cm]. In order to better suit the specifications of the beam shaping lens the beam diameter was reduced with two lenses in a telescope configuration. In Figure 6 CCD captions of the beam profile with and without the addition of the beam shaping optics are presented. As can be clearly seen, the intensity profile produced by the top-hat lens is not homogeneous, this is due to our gaussian beam diameter not matching completely the design one. Nevertheless we can take advantage of the features of our profile to

confirm that wathever the intensity map is the crystalline mark will have the same distribution. The profile also changes with the defocus.

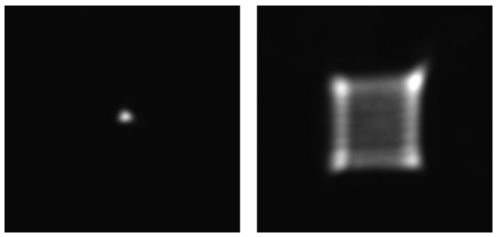

Figure 6. In-focus beam profiles. Left: Without top-hat lens. Righ: With top-hat lens

Several pulses were shot in a 100 nm thick layer of GST grew on SiO_2 for different input power and defocus of the sample. In Figure 7 the crystalline mark produced by a in-focus single pulse of approximately 7.7 μm/cm^2 of fluence is shown as observed with a microscope in transmission configuration. An overlap of the crystalline mark and the beam profile after adjusting the scales of both images is also presented.

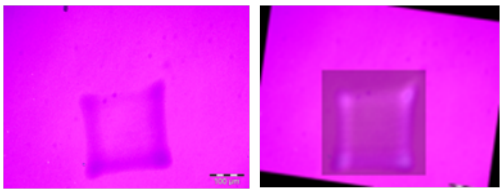

Figure 7. Left: Image of the crystalline mark formed after a single laser pulse. Right: Overlap of the crystalline mark and the beam profile

As it was expected from our simulations, the crystalline mark reproduces with great precission the beam profile, this was confirmed also with the line scans of both pictures. The relative change in transmissivity is up to 20% in the darker areas. This value sits close to the case of full crystallization clearly exceeding our predictions, however, a more detailed study of transmission propierties would be needed to correclty estimate the crystalline fraction in the GST layer.

5. Conclusion

We have clarified that lateral thermal diffusion is not a factor in the resolution of crystalline marks produced in amorphous GST under femtosecond illumination. This is true for all the cappings and substrates commonly used for GST. In addition this result can be extended to longer pulses as long as the deposition of heat happens before thermalization, since the following dynamics will be the same. This highlights an advantage of sub-nanosecond optical switching versus slower pulsed optical or electrical switching, since the pulses can't achieve a fast enough introduction of heat there will be a build up of temperature outside the initial heated zone as a result of the presence of

a heat source in the thermalization process, limiting the ability to shape the crystalline marks.

6. bibliography

[1] M. M. Aziz, M. R. Belmont, and C. D. Wright. Ultrafast heating and resolution of recorded crystalline marks in phase-change media. *Journal of Applied Physics*, 104(10), 2008.

[2] Kenneth E. Goodson Elah Bozorg-Grayeli, John P. Reifenberg, Mehdi Asheghi, H.-S. PhilipWong. Thermal Transport in Phase Change Memorymaterials. *Annual Review of Heat Transfer*, 16:397–428, 2013.

[3] Rakesh Jeyasingh, Scott W. Fong, Jaeho Lee, Zijian Li, Kuo Wei Chang, Davide Mantegazza, Mehdi Asheghi, Kenneth E. Goodson, and H. S Philip Wong. Ultrafast characterization of phase-change material crystallization properties in the melt-quenched amorphous phase. *Nano Letters*, 14(6):3419–3426, 2014.

[4] Duygu Kuzum, Rakesh G D Jeyasingh, Byoungil Lee, and H Philip Wong. Materials for Brain-Inspired Computing. pages 2179–2186, 2012.

[5] Peining Li, Xiaosheng Yang, Tobias W. W. Maß, Julian Hanss, Martin Lewin, Ann-Katrin U. Michel, Matthias Wuttig, and Thomas Taubner. Reversible optical switching of highly confined phononpolaritons with an ultrathin phase-change material. *Nature Materials*, (May), 2016.

[6] Y. Liu, M. M. Aziz, A. Shalini, C. D. Wright, and R. J. Hicken. Crystallization of Ge2Sb2Te5 films by amplified femtosecond optical pulses. *Journal of Applied Physics*, 112(12), 2012.

[7] J. Orava, A. L. Greer, B. Gholipour, D. W. Hewak, and C. E. Smith. Ultra-fast calorimetry study of Ge2Sb2Te5 crystallization between dielectric layers. *Applied Physics Letters*, 101(9):091906, 2012.

[8] M Praprotnik, M Sterk, and R Trobec. Inhomogeneous heat-conduction problems solved by a new explicit finite difference scheme. *International Journal of Pure and Applied Mathematics*, 13(3):275–291, 2004.

[9] Miquel Rudé, Robert E. Simpson, Romain Quidant, Valerio Pruneri, and Jan Renger. Active Control of Surface Plasmon Waveguides with a Phase Change Material. *ACS Photonics*, 2(6):669–674, 2015.

[10] J. Siegel, W. Gawelda, D. Puerto, C. Dorronsoro, J. Solis, C. N. Afonso, J. C. G. de Sande, R. Bez, a. Pirovano, and C. Wiemer. Amorphization dynamics of Ge[sub 2]Sb[sub 2]Te[sub 5] films upon nano- and femtosecond laser pulse irradiation. *Journal of Applied Physics*, 103(2):023516, 2008.

[11] Lutz Waldecker, Timothy a. Miller, Miquel Rudé, Roman Bertoni, Johann Osmond, Valerio Pruneri, Robert E. Simpson, Ralph Ernstorfer, and Simon Wall. Time-domain separation of optical properties from structural transitions in resonantly bonded materials. *Nature Materials*, 14(July):1–6, 2015.